Desalination and Water Treatment
www.deswater.com

doi: 10.5004/dwt.2022.28137

257 (2022) 34–40
May

Surface characterization and interfacial analysis of organic membranes: an investigation on electrical and wettability phenomenon

Hassna Laalaoua[a,*], Youssef Amine Boussouga[a], Oumaima Nahid[a], Safae Er Raouan[b], Saad Ibnsouda Koraichi[b], Abdelhadi Lhassani[a]

[a]*Laboratory of Processes Materials and Environment, Faculty of Science and Technology of Fez, Sidi Mohamed Ben Abdellah University, P.O. Box: 2202, Fez, Morocco, Tel. +212658611341; emails: hassna.laalaoua94@gmail.com (H. Laalaoua), boussouga.youssef@gmail.com (Y.A. Boussouga), oumaima.nahid@usmba.ac.ma (O. Nahid), abdelhadi.lhassani@usmba.ac.ma (A. Lhassani)*
[b]*Laboratory of Microbial Biotechnology, Department of Biology, Faculty of Science and Technology of Fez, Sidi Mohamed Ben Abdellah University, P.O. Box: 2202, Fez, Morocco, emails: serraoan@gmail.com (S. Er Raouan), saad.ibnsouda@usmba.ac.ma (S.I. Koraichi)*

Received 30 May 20021; Accepted 4 January 2022

ABSTRACT

The characterization of membrane properties represents an essential step towards the understanding and prediction of membrane filtration performance. Herein, surface properties of commercial polymeric membranes were investigated in terms of surface charge and wetting characteristics. Streaming potential measurements showed that the studied membranes (NF270, NF90, BW30LE and BW30) were negatively charged in electrolytic solutions at neutral pH which is related to the polymeric composition of the active layer. Contact angle measurements were performed to evaluate qualitatively the wettability/hydrophilicity of the membranes and quantitatively by evaluating electron donor and acceptor functionalities and interfacial free energies of each membrane surface. NF270 was the most hydrophilic membrane with a high wettability degree (θ = 33.2°, $-\Delta G_{Sw}$ = 133.55 mJ/m^2), Furthermore, the wettability parameters were correlated to membrane permeability, in order to better understand the wetting/hydrophilic behavior. This study on the electrical and wettability properties are of importance to select the appropriate membrane prior operation where the performance is related to the surface characteristics.

Keywords: Nanofiltration; Reverse osmosis; Surface characterization; Streaming potential; Contact angle; Interface analysis; Wettability

1. Introduction

Membrane separation is recognized as a promising technology for gas separation [1], water desalination [2], as well as agrifood and pharmaceutical industry [3–5]. Membrane surface properties are of great importance to control separation performance, especially solute-water selectivity (A variety of NF and RO membranes exists, each membrane have its own specific characteristics and performance. The relationship between the membrane performance and the membrane characteristics is still not clear and to study this relationship a detailed membrane characterization is needed. For example, membrane charge functionality influences on the distribution of ions in the solution due to requirement of the electroneutrality of the system [6]. Membrane surface hydrophilicity impacts on the membrane permeability [7] and fouling [8]. The surface morphology of membranes can help to explain fouling phenomenon during separation processes [9,10].

* Corresponding author.

Presented at the Second International Symposium on Nanomaterials and Membrane Science for Water, Energy and Environment (SNMS-2021), June 1–2, 2022, Tangier, Morocco

In literature, streaming potential measurement is the most common method to evaluate surface charge characteristics of polymeric membranes [11–13]. On the other hand, contact angle method is useful to study the degree of wettability/hydrophilicity of polymeric membranes, knowing that more hydrophilic membrane provides a better permeability [14]. Although, hydrophilicity can be influenced by the roughness of the membrane surface. For this, atomic force microscopy (AFM) technique was used to study membrane surface morphology and its effect on degree of hydrophilicity [15,16].

The objective of this study was to investigate the surface of polymeric composite NF/RO membranes regarding; (i) surface charge of membrane using streaming potential (SP) method, and (ii) membrane hydrophilicity through contact angle measurements which are useful for evaluating solid surface tension components (electron donor and electron acceptor functionality) and interfacial free energies of adhesion and cohesion using Lifshitz–van der Waals/acid–base approach. Contact angles results of the studied NF and RO membranes were matched with membrane permeability experiments with pure water which has been made on a cross-flow filtration process at laboratory scale. This fundamental study presents a comprehensive characterization of two NF membranes denoted NF90, NF270 and two RO membranes denoted BW30 and BW30LE, by their wettability and surface charge parameters.

2. Materials and methods

2.1. Membrane choice and characterization

The membranes selected for this study were provided by DuPont (USA), namely NF270, NF90, BW30 and BW30LE. These polymeric membranes are of asymmetric and thin-film composite type, the active layer is deposited with polyamide on microporous polysulfone support, through a binding layer of polysulfone. According to the manufacturer, the characteristics of these membranes are summarized in Table 1.

Before each characterization, all membranes were reconditioned for 24 h with ultrapure water (pH = 6.4, $\lambda < 1$ μs). In the case of contact angle measurements, membrane samples were dried after reconditioning at room temperature (24°C) in a desiccator. For filtration experiments, the membranes were compacted with ultrapure water prior permeability measurements.

2.2. Streaming potential measurements

The streaming potential (SP) measurements were performed in flow through mode. The filtration cell (Model 8050, Amicon, Millipore, France), with a capacity of 50 mL, was used for a membrane coupon with an effective filtration area of 14.52 cm^2. The unit was operated at pressure up to 5 bar using pressurized nitrogen gas as a driving force. A pair of Ag/AgCl electrodes introduced in the cell was used to measure the potential difference between both sides (feed and permeate) of the membrane as a function of the pressure applied. The electrodes were connected to a voltmeter (PHM250 from Radiometer Analytical, France) with high impedance (10 MΩ). The positive potential was connected to the feed and the negative one to the permeate. The experiment was done at room temperature of 20°C. The streaming potential was measured in 1 mM of KCl solution at different pH in order to estimate the membrane isoelectric point (IEP). The pH was adjusted by adding HCl or NaOH to the solutions and was varied in the range from 2 to 10.

The (SP), which is linked to the zeta potential, was calculated by Helmholtz–Smoluchovsky equation [19]:

$$SP = \frac{\Delta\phi}{\Delta P} = \frac{\varepsilon\xi}{\mu\chi} \quad (1)$$

where $\Delta\phi$ is the transmembrane potential difference, ΔP is the trans-membrane pressure, ε is the permittivity, ξ is the zeta potential, μ is the dynamic viscosity, χ is the ionic conductivity of the electrolyte solution (1 mM KCl). The linear relation between $\Delta\phi$s and ΔP represents the coefficient of streaming potential (SP).

The streaming potential method is the most useful way to determine qualitatively the charge of a porous polymeric membrane as reported recently

2.3. Contact angle measurements

The contact angle measurements were performed through the sessile drop method by using a Goniometer

Table 1
Characteristics of the polyamide thin-film composite NF/RO membranes as specified by the manufacturer

Membrane	Maximum temperature (°C)	Maximum pressure (bar)	pH range	Rejection (%)			Molecular weight cut off (Da)	Roughness (nm) 50 μm × 50 μm [17]
				NaCl	$MgSO_4$	$CaCl_2$		
NF270[a]	45	41	3–10	–	>97	40–60	~200–400	45 ± 5
NF90[b]	45	41	3–10	85–95	>97	–	~200–400	71 ± 5
BW30LE[c]	45	41	2–11	99.3	–	–	~100	283 ± 10
BW30[d]	45	41	2–11	99.5	–	–	~100	290 ± 10

[a]Test conditions: 0.5 g/L $CaCl_2$, 2.0 g/L $MgSO_4$, 15% recovery, operating pressure 4.8 bar, 25°C [18].
[b]Test conditions: 2.0 g/L NaCl, 2.0 g/L $MgSO_4$, 15% recovery, operating pressure 4.8 bar, 25°C [18].
[c]Test conditions: 2.0 g/L NaCl, 15% recovery, operating pressure 10.3 bar, pH 8, 25°C [18].
[d]Test conditions: 2.0 g/L NaCl, 15% recovery, operating pressure 15.5 bar, pH 8, 25°C [18].

DGD-MCAT (France) with an environmental chamber. For the determination of surface tension components and interfacial free energies of the solid surface, two polar liquids (pure water and formamide) and one non-polar liquid (diiodomethane) were used with known surface tension characteristics (Table 2). The contact angle of each liquid was measured from the steady-state values which were typically observed after 30 s. Sessile drop contact angles for each liquid were measured as the angle between the baseline of a liquid drop and the tangent at the solid–liquid boundary. The room temperature was about 20°C. For statistical analysis, data were expressed as mean ± standard error and analyzed using SPSS Statistics 22 software by one-way ANOVA followed by Tukey post hoc test with significance defined at $p < 0.05$.

2.3.1. Surface tension and interfacial compounds

As firstly described by Young [23], the angle of contact (θ) of a liquid fall on a solid surface is defined by the mechanical equilibrium of the drop under the action of three interfacial tensions; solid–liquid γ_{SL}, solid–vapor γ_{SV} and liquid–vapor γ_{LV}. At equilibrium, the sum of the three forces applied to the surface is zero. This leads to Young's equation:

$$\gamma_{LV}\cos\theta = \gamma_{SV} - \gamma_{SL} \tag{2}$$

Oss et al. [24] proposed a generalization of the Fowkes approach to surface tension components, also called the Lifshitz–van der Waals/acid–base approach which is described as follows:

$$\gamma_i = \gamma_i^{LW} + \gamma_i^{AB} \tag{3}$$

$$\gamma_i^{AB} = 2(\gamma_i^+\gamma_i^-)^{1/2} \tag{4}$$

The interfacial tension between the solid (S) and liquid (L) phases are described by the following equation:

$$\gamma_{SL} = \gamma_S + \gamma_L - 2\left(\gamma_S^{LW}\gamma_L^{LW}\right)^{1/2} - 2\left(\gamma_S^+\gamma_L^-\right)^{1/2} - 2\left(\gamma_S^-\gamma_L^+\right)^{1/2} \tag{5}$$

where γ^{LW} is the Lifshitz–van der Waals component, γ^- and γ^+ are the electron donor (Lewis base) and acceptor (Lewis acid) surface tension components, respectively, in the *i* phase.

Under the assumption of negligible vapor adsorption ($\gamma_{LV} \approx \gamma_L$) [25], the combination of Young's equation Eq. (2) with Eq. (5) leads to Eq. (6) which known as the extended Young–Dupré equation [26]:

$$\gamma_L(\cos\theta + 1) = 2\left(\gamma_S^{LW}\gamma_L^{LW}\right)^{1/2} + 2\left(\gamma_S^+\gamma_L^-\right)^{1/2} + 2\left(\gamma_S^-\gamma_L^+\right)^{1/2} \tag{6}$$

Eq. (6) can be solved simultaneously using measured contact angles from one apolar and two polar liquids with known values of γ^{LW}, γ^-, and γ^+.

2.3.2. Solid–liquid interfacial free energy

The solid–liquid interfacial free energy (ΔG_{SL}) between a solid (or a condensed-phase substance) S and a polar liquid L in air or in vacuo must be evaluated using Eq. (7) [26], as follows:

$$\begin{aligned}\Delta G_{SL} &= \gamma_{SL} - \gamma_S - \gamma_L \\ &= -2\left(\sqrt{\gamma_S^{LW}\gamma_L^{LW}} + \sqrt{\gamma_S^+\gamma_L^-} + \sqrt{\gamma_S^-\gamma_L^+}\right)\end{aligned} \tag{7}$$

This parameter gives a fundamental insight about the wettability of a material in contact with water [27].

2.3.3. Interfacial free energy of cohesion

The free energy of cohesion (or interaction) ΔG_{SLS} between two identical molecules or particles of S, the membrane material in this case, dissolved or immersed in a polar liquid L (e.g., water) can be expressed by the following equation [26,28]:

$$\begin{aligned}\Delta G_{SLS} &= -2\gamma_{SL} \\ &= -2\left[\left(\left(\gamma_S^{LW}\right)^{1/2} - \left(\gamma_L^{LW}\right)^{1/2}\right)^2 + 2\left(\begin{matrix}\left(\gamma_S^+\gamma_L^-\right)^{1/2} + \left(\gamma_L^+\gamma_L^-\right)^{1/2} - \\ \left(\gamma_S^+\gamma_L^-\right)^{1/2} - \left(\gamma_L^+\gamma_S^-\right)^{1/2}\end{matrix}\right)\right]\end{aligned} \tag{8}$$

This approach allowed us to evaluate the degree of hydrophobicity of each membrane surface. If the free energy is positive, a material may be considered hydrophilic when immersed in water, and if the free energy is negative the material is hydrophobic [29].

In this work, ΔG_{SL} and ΔG_{SLS} were calculated using surface tension characteristics of pure water, the term "L" will be replaced by "W" in results and discussion section.

2.4. Membrane permeability experiments

Permeability experiments were carried out at bench-scale cross flow set-up equipped with a membrane filtration cell (Osmonics, Module SEPA CFII, USA) with an active filtration area of 138 cm^2. The cell is equipped with a hydraulic clamping system to work up to 69 bars of pressure. A HP pump (Wanner, USA) with a feeding circulation speed regulator was used for pressure. Two valves were installed at the outlet (concentrate) and the inlet (feed) to control the applied pressure and the recovery. Feed and concentrate flow rates were measured with two flow meters (Omega, USA). The total volume of the system is 5 L and a thermostat to set the desired temperature.

Table 2
Surface tension properties of pure liquids used for contact angle measurements [22]

Liquids	Surface tension properties (mJ/m^2) at 25°C		
	γ^{LW}	γ^+	γ^-
Water (H_2O)	21.8	25.5	25.5
Formamide (CH_3NO)	39.0	2.3	39.6
Diiodomethane (CH_2I_2)	50.5	0.0	0.0

The permeability (L_p) of the membranes was calculated using Eq. (9):

$$J_v = L_p \Delta P \quad (9)$$

where J_v is the permeate flowrate.

3. Results and discussions

3.1. Membrane permeability

In order to better justify the wettability behavior of the selected NF/RO membranes, permeability tests were required through the application of Eq. (9). The results of hydraulic permeability (L_p) of pure water are provided in Table 3. According to these results and as expected NF membranes were more permeable than the RO membranes. The difference in permeability is directly related to their MWCO/pore size. This is true for NF270, which has the highest pore size compared to the tight NF90 membrane [30]. Hydraulic permeability results of the studied NF/RO membranes were different from those reported in the literature [31–36] which can be explained by the different system used for characterization. The variation of pure water flux as a function of the applied pressure for the NF and RO studied membranes are plotted in Fig. 1.

3.2. Surface charge and isoelectric point determination

The surface charge of the studied NF and RO membranes was evaluated by streaming potential measurements through the application of Eq. (1). The variation of streaming potential coefficient (SP) as function of pH for NF270, NF90, BW30LE and BW30 membranes were plotted as shown in Fig. 2. In addition, this technique allowed us to determine the isoelectric point (IEP) for each membrane which is the pH at which the membrane has a neutral charge (Table 4).

The membrane charge is relative to the protonation/deprotonation of functional groups present in the active layer, which can be affected by the charge shielding in electrolyte solutions [37–40]. The active layer of the selected membranes (NF270, NF90, BW30, BW30LE) consists of polyamide with carboxyl and amine functional groups [41]. By passing from the acid to the alkaline medium, the active layer of these membranes exhibits chemical changes. Positive surface charge results from protonation of the amine groups at lower pH [41,42]. On the other hand, the negative surface charge results from the deprotonation of the carboxylic groups at higher pH [41,42]. The isoelectric point for these membranes was located between 2.6 and 5.5. The position of the isoelectric point is similar for the BW30 and BW30LE membranes. The values of isoelectric point found for the NF270 (2.6) and NF90 (4.3) are not quite far from those found in other studies

3.3. Wettability/hydrophilicity of membranes

The contact angles of the studied NF and RO membranes were measured with pure water, formamide and diiodomethane as listed in Table 5. The contact angles with pure water reflect the membrane surface hydrophilicity, which is mainly controlled by electrostatic and/or hydrogen-bond interactions between the water molecules and surface functional groups of the active layer [12]. Contact angle values with pure water of the studied NF/RO membranes were lower than 90° which means that they have hydrophilic surface. The hydrophilicity, in the case of these polyamide membranes, is related to the presence of

Table 3
Hydraulic permeability with pure water (L_p) for the studied NF and RO membranes

NF/RO	Hydraulic permeability (L/h bar m²)		
	In this work	In the literature	
NF270	5.48	5.1–14.86	[32,34]
NF90	4.44	6.05–11.2	[31,33]
BW30LE	4.11	2.77–5.32	[35,36]
BW30	2.45	1.97–3.50	[32,33]

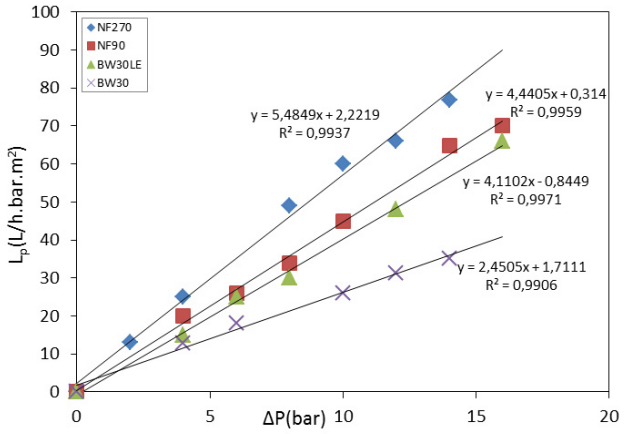

Fig. 1. Pure water flux as a function of the applied pressure for the NF and RO membranes (T = 24°C, pH = 6.4, λ < 1 µs).

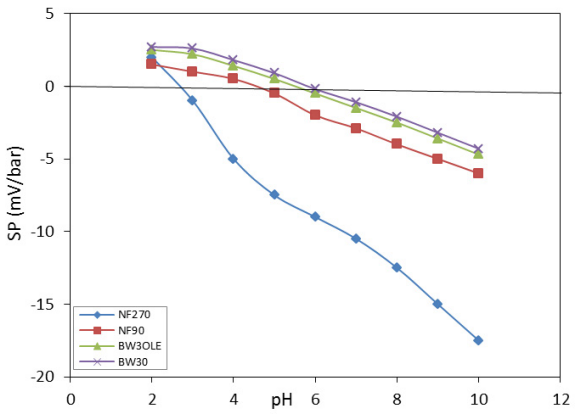

Fig. 2. The behavior of streaming potential coefficient (SP) as function of pH for the studied NF/RO membranes (KCl = 1 mM, T = 20°C).

Table 4
Isoelectric point (IEP) of the studied NF and RO membranes

Membrane type	NF270	NF90	BW30LE	BW30
Charge (neutral pH)	Negative	Negative	Negative	Negative
IEP (KCl 1 mM) (±0.3)	2.6	4.3	5.2	5.5

Table 5
Summary of contact angles of NF and RO membranes measured by the sessile drop method at 20°C

Membrane	Contact angle θ (°)				
	Pure water	Pure water	In the literature	Formamide	Diiodomethane
NF270	33.2 ± 0.96	28.0 – 51.4	[34,47,49]	31.2 ± 1.16	59.5 ± 0.78
NF90	45.2 ± 0.37	11.0 – 67.5	[12,34,47,48]	21.4 ± 0.8	64.2 ± 0.59
BW30LE	53.3 ± 0.56	42.0 – 87.6	[31,45,50]	41.6 ± 0.55	43.9 ± 0.46
BW30	58.0 ± 1.26	43.8 – 76.0	[19,34,46,47]	31.4 ± 1.23	56.3 ± 0.79

Table 6
Surface tension components (Lifshitz–van der Waals (γ^{LW}), Lewis acid (γ^{+}) and Lewis base (γ^{-})) and interfacial free energies (of adhesion ΔG_{Sw} and cohesion ΔG_{SwS}) of NF and RO membranes

Membrane type	Surface tension: components and parameters (mJ/m^2)				
	γ^{LW}	γ^{+}	γ^{-}	$-\Delta G_{Sw}$	ΔG_{SwS}
NF270	28.9 ± 0.45	2.6 ± 0.22	44.1 ± 1.85	133.55	20.95
NF90	26.2 ± 0.34	7.0 ± 0.36	24.2 ± 0.61	124.20	–1.46
BW30LE	37.6 ± 0.21	0.6 ± 0.11	25.9 ± 1.10	116.48	–3.23
BW30	30.7 ± 0.46	4.6 ± 0.59	14.1 ± 1.81	111.32	–16.07

carboxylic and amine groups capable to interact with water molecules by hydrogen-bond [12,16].

Generally, the lower is the contact angle the more hydrophilic is the material [14]. This is true for the case of NF270 membrane. As shown in Table 5, the contact angles differ significantly from those mentioned in the literature differences might result from various factors, such as temperature, humidity, measurement time, drop volume, water purity and the measurement method.

Solid surface tensions and interfacial free energies (Table 6) of the investigated NF/RO membranes were derived through van Oss et al. [51]. Method by using contact angle values of pure water, formamide and diiodomethane from Table 5.

Quantitative analysis of membrane surface tension and interfacial free energy through contact angle measurements showed that the studied membranes have both polar functionalities (electron donor and electron acceptor) with fairly low interfacial free energy, which are consistent with the studied polyamide RO/NF membranes in literature [27,49]. According to van Oss experiments, a value of $\gamma^{(-)}$higher than 27.9 mJ/m^2 represent a hydrophilic surface, while the opposite case indicates a hydrophobic surface. In addition, a positive surface free energy represents a hydrophilic surface, whereas the negative value represents a hydrophobic surface [52]. The surface of NF270 membrane was more electron donor rich ($\gamma^{(-)}$ > 27.9 mJ/m^2) wetted ($-\Delta G_{Sw}$ = 133.55 mJ/m^2) and hydrophilic (ΔG_{SwS} > 0), compared to the other membrane surfaces (NF90, BW30LE and BW30) which have electron donor character values less than 27.9 mJ/m^2 and negative values of ΔG_{SwS} resulting in low wettability/hydrophilicity degrees. The surface of NF270 has comparable contact angle with water, this membrane is the most hydrophilic membrane. The most hydrophobic membranes are the NF90, BW30 and BW30LE.

From Fig. 3 it is seen that the better wettability/hydrophilicity degree in NF270 membrane is explained by the highest value of $-\Delta G_{Sw}$ and the lowest value of contact angle, this has resulted in a better permeability of the membrane comparing to NF90 and the studied RO membranes.

4. Conclusions

Electrical surface charge characterization by using streaming potential method, has shown that all studied membranes were negatively charged at neutral pH due to their polymeric composition (polyamide). Contact angle measurements on the investigated NF/RO membrane allowed us to get better understanding of their wettability. Analysis of membrane surface tensions and interfacial free energy using contact angles value from pure water, formamide and diiodomethane, has shown that NF270 membrane was the most hydrophilic membrane (θ = 33.2°) and higher wettability ($-\Delta G_{Sw}$ = 133.55 mJ/m^2) with a positive

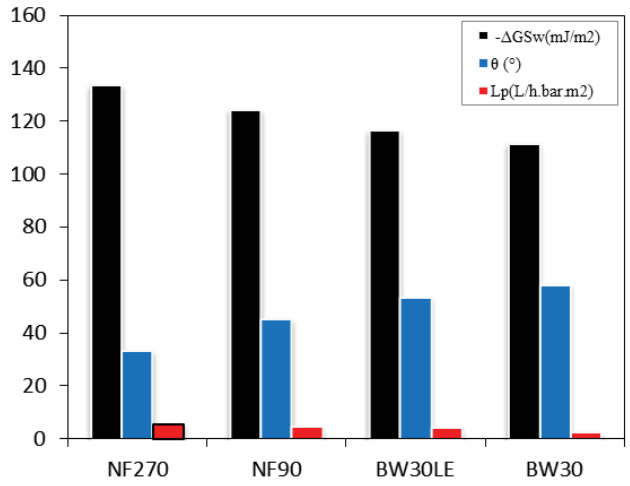

Fig. 3. NF/RO membranes proprieties regarding contact angle (θ), $-\Delta G_{Sw}$ and permeability (L_p)

value of the interfacial free energy (ΔG_{SwS} = 20.95 mJ/m^2). This was in contrast to NF90, BW30LE and BW30 which had negative values of the interfacial free energy ($\Delta G_{SwS} < 0$). These results were confirmed by permeability experiments in which the NF270 was the most permeable membrane (L_p = 5.48 L/h/m^2). In addition, the surface characteristics of NF90 were fairly close to BW30 and BW30LE which can make this membrane more selective.

Symbols

ΔP	—	Transmembrane pressure
$\Delta\phi$	—	Transmembrane potential difference
ε	—	Permittivity
ξ	—	Zeta potential
μ	—	Dynamic viscosity
χ	—	Ionic conductivity
θ	—	Contact angle
MWCO	—	Molecular weight cut–off
γ_{SL}	—	Interfacial tension solid–liquid
γ_{SV}	—	Interfacial tension solid–vapor
γ_{LV}	—	Interfacial tension liquid–vapor
γ^+	—	Surface tension acid
γ^-	—	Surface tension base
γ^{LW}	—	Lifshitz–van der Waals surface tension
ΔG_{SL}	—	Solid–liquid interfacial free energy
ΔG_{SLS}	—	Free energy of cohesion (or interaction)
J_v	—	Permeate flow
L_p	—	Hydraulic permeability

References

[1] S. Kim, T.W. Pechar, E. Marand, Poly(imide siloxane) and carbon nanotube mixed matrix membranes for gas separation, Desalination, 192 (2006) 330–339.

[2] K. Gethard, O. Sae-Khow, S. Mitra, Water desalination using carbon-nanotube-enhanced membrane distillation, ACS Appl. Mater. Interfaces, 3 (2011) 110–114.

[3] B. Tylkowski, B. Trusheva, V. Bankova, M. Giamberini, G. Peev, A. Nikolova, Extraction of biologically active compounds from propolis and concentration of extract by nanofiltration, J. Membr. Sci., 348 (2010) 124–130.

[4] Q. Fan, K.K. Sirkar, B. Michniak, Iontophoretic transdermal drug delivery system using a conducting polymeric membrane, J. Membr. Sci., 321 (2008) 240–249.

[5] I.H. Tsibranska, B. Tylkowski, Concentration of ethanolic extracts from *Sideritis* ssp. L. by nanofiltration: comparison of dead-end and cross-flow modes, Food Bioprod. Process., 91 (2013) 169–174.

[6] J. Schaep, C. Vandecasteele, Evaluating the charge of nano-filtration membranes, J. Membr. Sci., 188 (2001) 129–136.

[7] G. Pearce, Introduction to membranes: membrane selection, Filtr. Sep., 44 (2007) 35–37.

[8] Y.L. Lin, Effects of organic, biological and colloidal fouling on the removal of pharmaceuticals and personal care products by nanofiltration and reverse osmosis membranes, J. Membr. Sci., 542 (2017) 342–351.

[9] W.R. Bowen, A.W. Mohammad, N. Hilal, Characterisation of nanofiltration membranes for predictive purposes – use of salts, uncharged solutes and atomic force microscopy, J. Membr. Sci., 126 (1997) 91–105.

[10] W.R. Bowen, J.A.G. Stoton, T.A. Doneva, Atomic force microscopy study of ultrafiltration membranes: solute interactions and fouling in pulp and paper processing, Surf. Interface Anal., 33 (2002) 7–13.

[11] C.Y. Tang, Y.-N. Kwon, J.O. Leckie, Probing the nano- and micro-scales of reverse osmosis membranes—a comprehensive characterization of physiochemical properties of uncoated and coated membranes by XPS, TEM, ATR-FTIR, and streaming potential measurements, J. Membr. Sci., 287 (2007) 146–156.

[12] J.V. Nicolini, C.P. Borges, H.C. Ferraz, Selective rejection of ions and correlation with surface properties of nanofiltration membranes, Sep. Purif. Technol., 171 (2016) 238–247.

[13] J. Lin, C.Y. Tang, C. Huang, Y.P. Tang, W. Ye, J. Li, J. Shen, R. Van Den Broeck, J. Van Impe, A. Volodin, C. Van Haesendonck, A. Sotto, P. Luis, B. Van der Bruggen, A comprehensive physico-chemical characterization of superhydrophilic loose nanofiltration membranes, J. Membr. Sci., 501 (2016) 1–14.

[14] Y. Baek, J. Kang, P. Theato, J. Yoon, Measuring hydrophilicity of RO membranes by contact angles via sessile drop and captive bubble method: a comparative study, Desalination, 303 (2012) 23–28.

[15] G.Z. Ramon, E.M.V. Hoek, Transport through composite membranes, part 2: impacts of roughness on permeability and fouling, J. Membr. Sci., 425–426 (2013) 141–148.

[16] Q. Li, X. Pan, Z. Qu, X. Zhao, Y. Jin, H. Dai, B. Yang, X. Wang, Understanding the dependence of contact angles of commercially RO membranes on external conditions and surface features, Desalination, 309 (2013) 38–45.

[17] M. Pontié, H. Dach, J. Leparc, M. Hafsi, A. Lhassani, Novel approach combining physico-chemical characterizations and mass transfer modelling of nanofiltration and low pressure reverse osmosis membranes for brackish water desalination intensification, Desalination, 221 (2008) 174–191.

[18] DOW, FILMTEC™ Membranes. Product Information Catalog, 2020. Available at: https://www.lennte ch.com/Data-sheets/Filmtec-Reverse-Osmosis-Product-Catalog-L.pdf

[19] K. Boussu, Y. Zhang, J. Cocquyt, P. Van der Meeren, A. Volodin, C. Van Haesendonck, J.A. Martens, B. Van der Bruggen, Characterization of polymeric nanofiltration membranes for systematic analysis of membrane performance, J. Membr. Sci., 278 (2006) 418–427.

[20] B.D. Coday, T. Luxbacher, A.E. Childress, N. Almaraz, P. Xu, T.Y. Cath, Indirect determination of zeta potential at high ionic strength: specific application to semipermeable polymeric membranes, J. Membr. Sci., 478 (2015) 58–64.

[21] P. Somovilla, J.P.G. Villaluenga, V.M. Barragán, Experimental determination of the streaming potential across cation-exchange membranes with different morphologies, J. Membr. Sci., 500 (2016) 16–24.

[22] H. Barkai, E. Soumya, M. Sadiki, B. Mounyr, K.S. Ibnsouda, Impact of enzymatic treatment on wood surface free energy: contact angle analysis, J. Adhes. Sci. Technol., 4243 (2016) 1–9.

[23] T. Young, An essay on the cohesion of fluids, Philos. Trans. R. Soc. London, (1805) 65–87, doi: 10.1098/rstl.1805.0005.

[24] C.J. Van Oss, M.K. Chaudhury, R.J. Good, Interfacial Lifshitz-van der Waals and polar interactions in macroscopic systems, Chem. Rev., 88 (1988) 927–941.
[25] D.Y. Kwok, D. Li, A.W. Neumann, Evaluation of the Lifshitz-van der Waals/acid–base approach to determine interfacial tensions, Langmuir, 10 (1994) 1323–1328.
[26] C.J. Van Oss, Development and applications of the interfacial tension between water and organic or biological surfaces, Colloids Surf., 54 (2007) 2–9.
[27] G. Hurwitz, G.R. Guillen, E.M.V. Hoek, Probing polyamide membrane surface charge, zeta potential, wettability, and hydrophilicity with contact angle measurements, J. Membr. Sci., 349 (2010) 349–357.
[28] J.A. Brant, A.E. Childress, Assessing short-range membrane–colloid interactions using surface energetics, J. Membr. Sci., 203 (2002) 257–273.
[29] C.J. Van Oss, The Properties of Water and Their Role in Colloidal and Biological Systems, Elsevier, 2008.
[30] Y.A. Boussouga, A. Lhassani, Modeling of fluoride retention in nanofiltration and reverse osmosis membranes for single and binary salts mixtures, Desal. Water Treat, 95 (2017) 162–169.
[31] C.Y. Tang, Y. Kwon, J.O. Leckie, Effect of membrane chemistry and coating layer on physiochemical properties of thin film composite polyamide RO and NF membranes II. Membrane physiochemical properties and their dependence on polyamide and coating layers, Desalination, 242 (2009) 168–182.
[32] H. Kelewou, A. Lhassani, M. Merzouki, P. Drogui, B. Sellamuthu, Salts retention by nanofiltration membranes: physicochemical and hydrodynamic approaches and modeling, Desalination, 277 (2011) 106–112.
[33] S. Yüksel, N. Kabay, M. Yüksel, Removal of bisphenol A (BPA) from water by various nanofiltration (NF) and reverse osmosis (RO) membranes, J. Hazard. Mater., 263 (2013) 307–310.
[34] M. Pontié, H. Dach, J. Leparc, M. Hafsi, A. Lhassani, Novel approach combining physico-chemical characterizations and mass transfer modelling of nanofiltration and low pressure reverse osmosis membranes for brackish water desalination intensification, Desalination, 221 (2008) 174–191.
[35] B. Teychene, G. Collet, H. Gallard, J.P. Croue, A comparative study of boron and arsenic(III) rejection from brackish water by reverse osmosis membranes, Desalination, 310 (2013) 109–114.
[36] A. Altaee, A. Sharif, A conceptual NF/RO arrangement design in the pressure vessel for seawater desalination, Desal. Water Treat., 3994 (2014) 1–13.
[37] A.E. Childress, M. Elimelech, Relating nanofiltration membrane performance to membrane charge (electrokinetic) characteristics, 34 (2000) 3710–3716.
[38] S. Bandini, C. Mazzoni, Modelling the amphoteric behaviour of polyamide nanofiltration membranes, Desalination, 184 (2005) 327–336.
[39] N. Saffaj, M. Persin, S. Alami Younssi, A. Albizane, M. Bouhria, H. Loukili, H. Dach A. Larbot, Removal of salts and dyes by low $ZnAl_2O_4$-TiO_2 ultrafiltration membrane deposited on support made from raw clay, Sep. Purif. Technol., 47 (2005) 36–42.
[40] J.A. Brant, K.M. Johnson, A.E. Childress, Characterizing NF and RO membrane surface heterogeneity using chemical force microscopy, Colloids Surf., A, 280 (2006) 45–57.
[41] N. Hilal, V. Kochkodan, H. Al Abdulgader, D. Johnson, A combined ion exchange-nanofiltration process for water desalination: II. Membrane selection, Desalination, 363 (2015) 51–57.
[42] M. Bauman, A. Košak, A. Lobnik, I. Petrinić, T. Luxbacher, Nanofiltration membranes modified with alkoxysilanes: surface characterization using zeta-potential, Colloids Surf., A, 422 (2013) 110–117.
[43] J. Tanninen, M. Mänttäri, M. Nyström, Effect of salt mixture concentration on fractionation with NF membranes, J. Membr. Sci., 283 (2006) 57–64.
[44] M. Mänttäri, A. Pihlajamäki, M. Nyström, Effect of pH on hydrophilicity and charge and their effect on the filtration efficiency of NF membranes at different pH, J. Membr. Sci., 280 (2006) 311–320.
[45] H. Dach, Comparison of Nanofiltration and Reverse Osmosis Processes for a Selective Desalination of Brackish Water Feeds, Engineering Sciences, Université d'Angers, USMBA of Fez, 2008.
[46] A. Simon, L.D. Nghiem, P. Le-Clech, S.J. Khan, J.E. Drewes, Effects of membrane degradation on the removal of pharmaceutically active compounds (PhACs) by NF/RO filtration processes, J. Membr. Sci., 340 (2009) 16–25.
[47] D. Norberg, S. Hong, J. Taylor, Y. Zhao, Surface characterization and performance evaluation of commercial fouling resistant low-pressure RO membranes, Desalination, 202 (2007) 45–52.
[48] A.M. Comerton, R.C. Andrews, D.M. Bagley, C. Hao, The rejection of endocrine disrupting and pharmaceutically active compounds by NF and RO membranes as a function of compound and water matrix properties, J. Membr. Sci., 313 (2008) 323–335.
[49] A. Subramani, E.M.V. Hoek, Direct observation of initial microbial deposition onto reverse osmosis and nanofiltration membranes, J. Membr. Sci., 319 (2008) 111–125.
[50] C. Wang, G.K. Such, A. Widjaya, H. Lomas, G. Stevens, F. Caruso, S.E. Kentish, Click poly(ethylene glycol) multilayers on RO membranes: fouling reduction and membrane characterization, J. Membr. Sci., 409–410 (2012) 9–15.
[51] C.J. van Oss, R.J. Good, R.J. Busscher, Estimation of the polar surface tension parameters of glycerol and formamide, for use in contact angle measurements on polar solids, J. Dispersion Sci. Technol., 11 (1990) 75–81.
[52] C.J. Van Oss, R.F. Giese, The hydrophilicity and hydrophobicity of clay minerals, Clays Clay Miner., 43 (1995) 474–477.